

# Status report on long-time decay measurements of $^{137}\text{Cs}$ radioisotope

Edit Fenyvesi<sup>a,b,\*</sup>, Gábor Gyula Kiss<sup>b</sup>, Dénes Molnár<sup>a</sup>, Péter Lévai<sup>a</sup> and Gergely Gábor Barnaföldi<sup>a</sup>

<sup>a</sup>HUN-REN Wigner Research Centre for Physics, Konkoly-Thege Miklós út 29-33., Budapest, 1121, Hungary

<sup>b</sup>HUN-REN Institute for Nuclear Research, Bem tér 18/c, Debrecen, 4026, Hungary

## ABSTRACT

The constancy of nuclear decay rates can be investigated via long-duration precision measurements. It is still an open question whether any (annual) modulation can be observed. Long-lasting nuclear decay rate measurements have been the subject of considerable research effort. A decay rate measurement with a  $^{137}\text{Cs}$  source is currently being conducted 30 meters below the ground at the Jánossy Underground Research Laboratory (JURLab, Csillebérc, Hungary) utilizing a High-purity Germanium (HPGe) detector. The laboratory is the low-radiation-background part of the Vesztergombi High Energy Laboratory (VLAB) on the KFKI campus, Csillebérc, Hungary. From October 2022 to April 2024, data of 18 months' worth have been collected, providing a new opportunity to look for variations in decay rates. The experimental setup, data processing method, and the first results of this measurement are presented here.

## 1. Introduction

One of the most elementary phenomena in nuclear physics is the law of nuclear decays, namely, the number of yet-undecayed nuclei drops exponentially with time as  $\sim \exp(-\lambda t)$ , where the decay constant,  $\lambda$  is characteristic to the specific nucleus. Tantalizing observations [1, 2, 3, 4, 5, 6, 7] suggest that the value of the *decay constant* might be modified by certain effects, therefore it is non-stationary. Such effects may be tiny but, nevertheless, might be observed by high-accuracy, long-lasting measurements in a monitored and controlled environment.

During the last decades, a lot of experimental and theoretical effort was dedicated to investigating various scenarios that possibly influence  $\beta$ -decay rates (i.e., decay half-lives). On the one hand, such effects would influence the treatment of nuclear waste; and on the other hand, those would have a strong impact also on nucleosynthesis processes taking place in dense and hot environments. Even just a few decades ago our knowledge of how the "external" environment affects  $\beta$ -decay half-lives was rather limited. The first attempts to study the dependence of the  $\beta$ -decay half-lives on magnetic field, temperature or pressure were carried out almost hundred years ago, but results showed negligible effects. However, in the middle of the 60's it was discovered that chemical effects can change the half-life of  $^7\text{Be}$  by 3.5% (for a review, see [8]).

In the second half of the 20<sup>th</sup> century, with the development of storage rings, related studies gained a new impetus due to the possibility of preserving highly ionized ions for longer times (potentially several hours) and following their decay. It was discovered that — due to the so-called "bound-state  $\beta$ -decay [9] — half-lives of highly charged ions can differ by several orders of magnitude from half-lives of the

corresponding neutral atoms. For example, a fully stripped  $^{187}\text{Re}^{75+}$  ion decays nine orders of magnitude faster than the neutral atom [10]. Another example is  $^{163}\text{Dy}$ , which is stable as a neutral atom but becomes radioactive, with  $t_{1/2} \approx 47$  days, when fully ionised to  $^{163}\text{Dy}^{66+}$ . The later case has a strong impact on the path of the astrophysical *s*-process synthesizing about 50% of the isotopes heavier than iron [11]. The physical basis of this effect is that the emitted  $\beta$ -particle (electron) is unable to access a bound final state and, therefore, it needs to be emitted with high kinetic energy, which is sometimes not possible because of energy conservation. A review of  $\beta$ -decay rate experiments carried out using storage rings can be found in Ref. [12].

The question of the constancy of the half-life also arose in the case of the electron capture decay mode. It is well-known that the low-energy laboratory cross sections of charged-particle fusion reactions are strongly affected by the so-called electron screening effect [13]. The electron cloud surrounding the target nucleus (which is typically in atomic form) reduces the Coulomb repulsion between the interacting nuclei and, as a result, larger cross sections are measured than the "real" ones. The effect can be characterized by an  $U_e$  screening potential. However, systematic measurements of the  $d(d,p)t$  reaction revealed that the screening potential becomes orders of magnitude higher (compared to the gas target value) when target nuclei are located in a metallic environment [14]. Different screening theories predict strikingly different changes to half-lives of the radioactive nuclei implanted into a metallic environment (and for the temperature dependence of half-lives). In the 2000's huge experimental efforts were devoted to study this effect and there is unresolved tension between the results of the different experiments even today [15, 16, 17, 18, 19, 20].

As discussed in the previous paragraphs, there are effects that can modify the half-life of beta decaying nuclei. The purpose of this work is to develop an experimental setup to investigate whether or not there is a periodic change in decay half-lives due to  $\beta$ -decay induced by solar electron neutrinos.

✉ fenyvesi.edit@wigner.hun-ren.hu (E. Fenyvesi)

🌐 <https://wigner.hu/infopages/fenyvesi.edit> (E. Fenyvesi)

ORCID(s): 0000-0003-2777-3719 (E. Fenyvesi); 0000-0002-6872-916X

(G.G. Kiss); 0009-0006-9345-9620 (P. Lévai); 0000-0001-9223-6480 (G.G. Barnaföldi)

Such an effect is expected to be tiny, however, it might be observed by high-accuracy, long-lasting measurements carried out in a low-background environment.

Historically, a remarkable oscillation in the relative decay rates of  $^{32}\text{Si}$  and  $^{36}\text{Cl}$  was reported in 1986 by an experiment at Brookhaven National Laboratory [1]. The period of oscillation was  $330 \pm 40$  days, consistent with an annual variation in decay rates, at a relative amplitude of few times  $10^{-3}$ . Similar observations have been made for other isotopes as well, such as  $^3\text{H}$  [3],  $^{238}\text{Pu}$  relative to  $^{56}\text{Mn}$  [2], and  $^{60}\text{Co}$  relative to  $^{90}\text{Sr}$ - $^{90}\text{Y}$  [4]. The origin of these decay rate variations is currently unknown. It has been suggested that the annual variation in the Sun's neutrino flux reaching Earth may play a crucial role, corresponding to Earth's slightly eccentric orbit and the resulting annual variation in the Sun-Earth distance [3]. However, even if neutrinos are responsible, the observed nuclear decay rates are too large to be explained by the Standard Model (SM) of particle physics because neutrinos interact in the SM far too weakly. Therefore, Beyond Standard Model physics is suspected [21, 22]. There might be a connection to Dark Matter as well as to the question of where neutrino masses come from, which similarly have no explanation within the Standard Model — yet are supported by observation. Experiments performed by Ephraim Fischbach's group at Purdue University have corroborated and extended these findings. First, they reconfirmed the annual oscillation in the  $^{32}\text{Si}/^{36}\text{Cl}$  relative decay rate found by the Brookhaven experiment. The Purdue group also measured oscillation components with non-annual periods, characteristic of solar physics [5]. In addition, decay rate anomalies associated with solar flares [6] were observed, and even a potential correlation with neutron star mergers was claimed [21]. So, besides potential insight into new physics, this line of experiments may lead to practical applications such as forecasting solar storms. However, these measurements were performed with outdated technology, and therefore come with sizable experimental uncertainties.

Compared to the experiments done at Purdue, the measurements described here allow higher precision due to far lower radioactive background at the underground facility; advanced, high-resolution HPGe detector technology (vs. NaI at Purdue); much better environmental controls (temperature, humidity) at JURLab. In this work, we present and analyze the decay data stability of a  $^{137}\text{Cs}$  radionucleus source, based on effectively six months of data taking between 7 October 2022 and 10 April 2024.

## 2. Measurements

In August 2021, a high-precision experimental program commenced to study nuclear decay rate anomalies at the Jánosy Underground Research Laboratory (JURLab) at the HUN-REN Wigner Research Center for Physics (HUN-REN Wigner RCP) [23]. This laboratory is a near-surface, low-radiation-background site at Csillebérc, Budapest, Hungary.

Figure 1 shows the timeline of the measurement, which includes data taking periods, graphs of the humidity and temperature vs. time, and the heating/ventilation/air conditioning (HVAC) system activity. We divide the measurement time line into continuous data taking periods ("Run"), which are listed in Table 1. Ideally, one would like to have a single long run of uninterrupted data taking but we had to strike a balance between running continuously and developing the detector system further (any change to the geometry ends a run). On occasion, the isotope had to be temporarily removed for administrative reasons (presented for inspection). Technical downtimes were rare and short but those do not affect the geometry anyway.

Shortly after an activation thick target yield measurement [24], we started with the Run-0 test period (from 7<sup>th</sup> July to 7<sup>th</sup> October 2022), including a long radiation background measurement in the JURLab. The test period was followed by Run-1 that started on 7<sup>th</sup> October 2022 and lasted until 24<sup>th</sup> March 2023. In this work we only present results based on data collected during Run-0 and Run-1.

### 2.1. Jánosy Underground Research Laboratory

The Jánosy Underground Research Laboratory (JURLab) is a special underground laboratory located 30 meters below ground (Fig. 2). This low-radiation-background facility is unique not only in Hungary but among the European Underground Laboratories (EUL) as well [25]. JURLab has three levels below the ground: a premise of 20 square meters at 10 meters depth (Level -1), two halls ( $2 \times 20$  square meters) at 20 meters depth (Level -2), three halls ( $2 \times 20$  square meters and 50 square meters) at 30 meters depth (Level -3).

The underground laboratory has electricity, ethernet, a preliminary laboratory gas system, and telephone lines. An uninterrupted power supply (UPS) unit provides electricity for the instruments of experiments going on in the laboratory. A HVAC ventilates the air at the facility. Normally, it operates for a few consecutive hours each week. Temperature can be kept constant to within  $\pm 0.2^\circ\text{C}$ , while relative humidity is constant to within  $\pm 5\%$  if the HVAC system is running continuously. This was, radon concentrations can be also reduced due to the air circulation. Furthermore, cosmic radiation is suppressed by 1-2 orders of magnitude compared to the surface-level radiation background.

The following measurements are going on in the laboratory: low radiation background measurement with a Canberra HPGe detector [23], muon tomography measurements with muon detectors [26], re-measurement of the Eötvös-experiment with a modernized Eötvös-balance [27, 28], and monitoring of seismicity with a Güralp seismometer and a Raspberry Shake 4D. A tiltmeter and an infrasound monitoring system are operating at the site. Since JURLab has multiple measurements ongoing in parallel, remote control is important to minimize human presence and any disturbance of the environment.

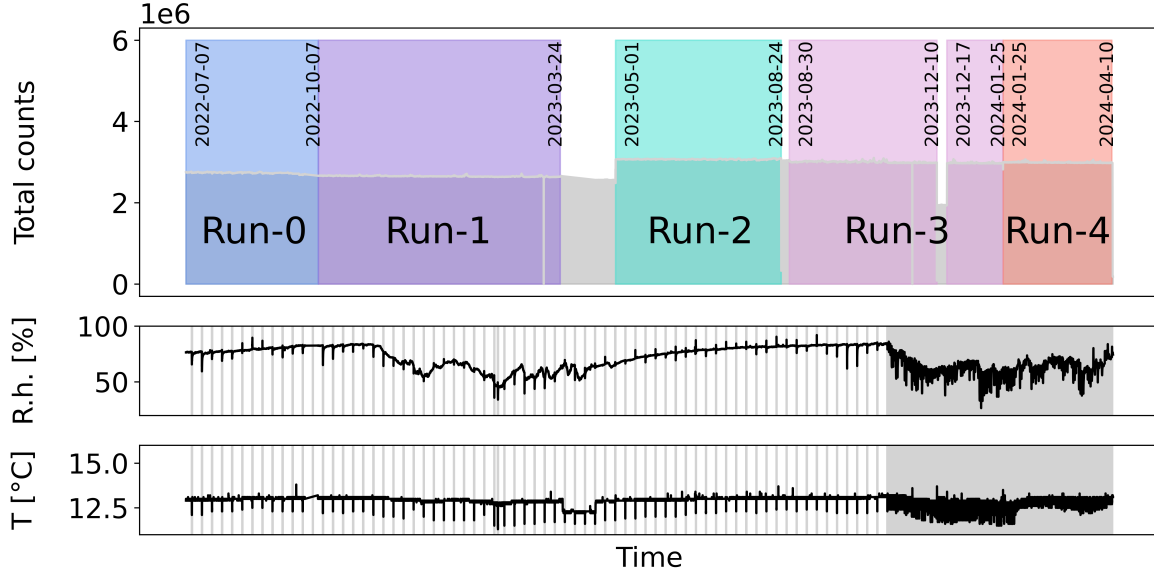


**Figure 1:** Timeline of the experiment, including total hourly counts in the detector during data taking periods (top plot, measurement runs indicated by shaded color bars), relative humidity (middle plot), temperature (bottom plot). HVAC system was used once a week until mid-Run-3, then daily until the end of Run-4 (shaded gray bars in the bottom two plots).

Run #	Start Date	End Date	Remark
Run-0	7 July 2022	7 October 2022	Test run: radio isotope positioning.
Run-1	7 October 2022	24 March 2023	Short DAQ system interrupt.
Run-2	1 May 2023	24 August 2023	Interruption: calibration of a signal generator.
Run-3	30 August 2023	25 January 2024	Measurement paused: the isotope was removed for checking.
Run-4	25 January 2024	10 April 2024	Experiment was stopped, the isotope was removed.

**Table 1**

Run periods of the measurement in the JURLab between 2022 and 2024.

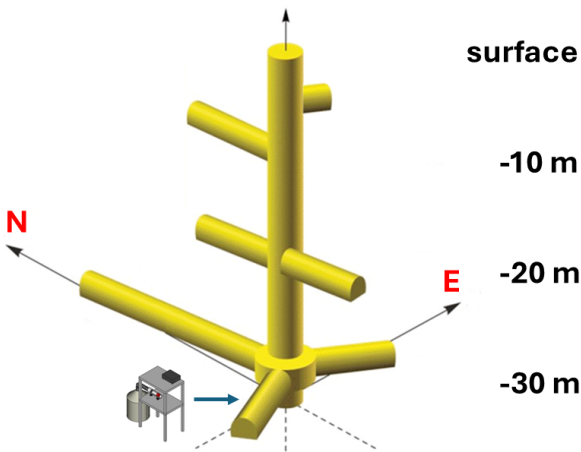


**Figure 2:** Measurement setup and structure of the HUN-REN Wigner Jánossy Underground Research Laboratory (JURLab).

## 2.2. Choice of radioisotope $^{137}\text{Cs}$

For our measurement, a  $^{137}\text{Cs}$  radioisotope was selected. The  $Q$  value and the half-life of this  $\beta$ -unstable isotope is

$Q_\beta = 1175.63$  keV and  $t_{1/2} = 30.08 \pm 0.09$  y. The  $\beta$ -decay predominantly ( $I_\beta = 94.7\%$ ) leads to the first excited state ( $E_x = 661.7$  keV) of the daughter nucleus ( $^{137}\text{Ba}$ ) after the emission of a  $\beta$ -particle ( $E_e^{max} = 513.97$  keV). The de-excitation to the ground state is followed by the emission of a single  $E_\gamma = 661.7$  keV energy  $\gamma$ -ray with  $I_\gamma = 85.1\%$ . The simple decay scheme, as well as the fact that the  $\beta$ -decay is accompanied by the emission of a single, higher-energy gamma transition than annihilation radiation, make the  $^{137}\text{Cs}$  isotope an ideal nucleus for our investigations. On the one hand side, the Compton background is lower above the 511 keV peak and thus the signal-to-noise ratio is better. On the other hand, because the decay is followed by the emission of a single  $\gamma$ -line, the so-called true coincidence summing effect is not present. The measurement was carried out using a sealed and calibrated  $^{137}\text{Cs}$  sources with activity of 155 kBq at the beginning of the measurement (7 July 2022).

The number of  $^{137}\text{Cs}$  nuclei is decreased in two ways:

- (i) by spontaneous decay:  $^{137}\text{Cs} \rightarrow ^{137}\text{Ba} + e^- + \bar{\nu}_e$  [29].

- (ii) the decay induced mainly by solar electron neutrinos: electron neutrinos interact with neutrons of the  $^{137}\text{Cs}$  nuclei:  $\nu_e + n^0 \rightarrow e^- + p^+$ , and can decrease the number of  $^{137}\text{Cs}$  nuclei via the reaction  $\nu_e + ^{137}\text{Cs} \rightarrow ^{137}\text{Ba} + e^-$ .

In the latter case, the above decays might be effected by the solar neutrino flux, which can vary according to the eccentricity of the orbit of Earth and the solar flare activity. Our plan is to investigate this phenomenon via a counting experiment at controlled environmental conditions with long-term monitoring.

### 2.3. Measurement setup and environment monitoring

The centerpiece of the experiment is a Canberra GC4018 high-purity germanium (HPGe) detector [30]. This is a  $p$ -type, coaxial detector, with an excellent resolution in the photon energy range  $\sim 40 \text{ keV} < \sim 10 \text{ MeV}$  of interest (full width half maximum  $\leq 0.87 \text{ eV}$  and  $\leq 1.80 \text{ keV}$  at energies  $122 \text{ keV}$  and  $1.33 \text{ MeV}$ , respectively, peak to Compton ratio  $\geq 62$ , and also good relative efficiency (40% or better). As photons traverse through the detector, they ionize the material and lose energy. The charge released is measured by the detector electronics and provides us (after calibration) with the photon energy. The experimental setup is shown in Fig. 3.

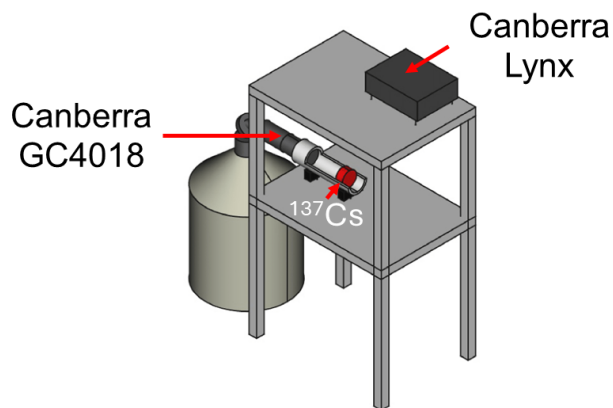


**Figure 3:** Measurement setup at Level -3 (depth of 30 m) in the JURLab.

To limit thermal noise during operation, HPGe detectors need to be cooled with liquid nitrogen (LN2) down to about  $77 \text{ K}$  ( $-196^\circ\text{C}$ ). The detector is sold as a single system together with a dipstick cryostat, which mainly consists of a 30-liter Dewar container. The Dewar stores enough nitrogen for about a week of operation, so it needs to be refilled periodically.

The data acquisition system (DAQ) is a Canberra Lynx Digital Signal Analyzer [31]. It has up to 32k channels, accurate time stamps, superior count rate and temperature stability, and ethernet connectivity. Data acquisition display and control, system energy/shape calibration and operation

of the digital oscilloscope are done via the HTTP interface of Lynx MCA. Spectral display, acquisition control, energy calibration and instrument setup are also possible using the built-in web server. So, except for liquid nitrogen fill-ups, one can run the entire experiment in standalone mode without any human presence.

The  $^{137}\text{Cs}$  sample is a small disk stored in a plastic holder, which is placed in a larger custom-made plastic holder disk. The large disk is standing in a custom-made holder which is manufactured from a hollow plastic cylinder. Part of the cylinder was removed, so the plastic holder disk can be placed into the trough (Fig. 4). The distance between the detector and the sample holder was kept fixed during the Run-1 data taking period.



**Figure 4:**  $^{137}\text{Cs}$  sample in front of the Canberra GC4018 high-purity germanium detector placed in a custom-made plastic holder. For the photo, lead shielding was partially removed to make the sample holder visible.

Temperature and relative humidity near the HPGe detector are monitored by an AM2315 sensor, which is connected to a Raspberry Pi computer that we used for periodic sensor readout (results were then transferred over ethernet for storage and analysis). In addition, humidity and temperature sensors of the HVAC system were also monitored remotely via ethernet. The temperature at the lowest level of JURLab was between  $12.2^\circ\text{C}$  and  $12.7^\circ\text{C}$  at nearly all times during Run-0 and Run-1 (cf. bottom panel of Fig. 1). The HVAC system of the facility typically operates for a few hours each Monday in order to remove humidity and radon from the laboratory. The time series of relative humidity measurements is plotted in the middle panel Fig. 1.

### 2.4. Data acquisition

Data collected by the Lynx analyzer are being saved to the cloud service of the HUN-REN Wigner Datacenter and the HUN-REN Wigner Scientific Computing Laboratory (WSCLAB), allowing for continuous monitoring and



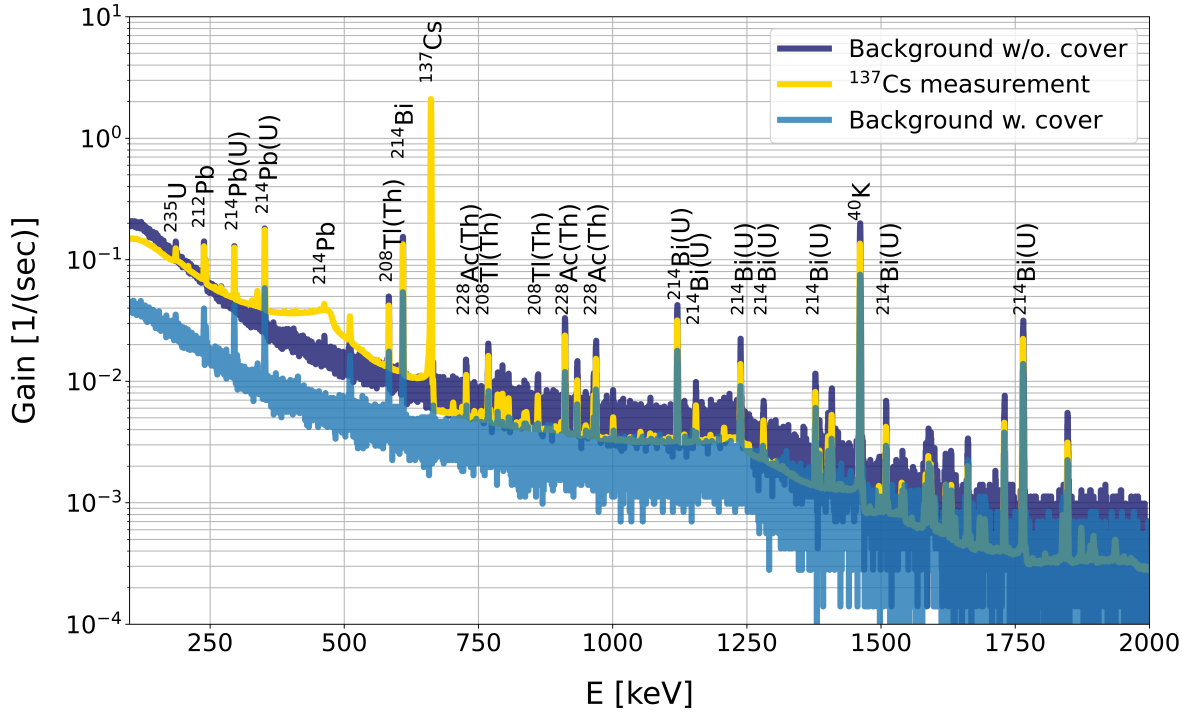


**Figure 5:** Gamma-ray spectra from HUN-REN Wigner Jánossy Underground Research Laboratory. Yellow line represents Run-1 of the  $^{137}\text{Cs}$  measurement. The light blue line represents the background with the lead covering used during Run-1, while the dark blue one represents the background without cover.

data analysis while the experiment is running. Primarily aggregate data have been stored, especially the photon spectra collected over one-hour "mini-run" intervals.

The gamma-spectra histograms were stored in 32768 bins. Linear energy calibration

$$E = A + B \times k \quad (1)$$

was applied, where  $k$  is the  $k^{\text{th}}$  channel of the DAC ( $0 \leq k \leq 32767$ ). Coefficients  $A = 0.07$  keV,  $B = 0.18$  keV/channel were calibrated to the  $^{214}\text{Pb}$  and  $^{40}\text{K}$  peaks at 351.93 keV and 1460.80 keV because those peaks stand out significantly above the background (Fig. 5). Calibration was performed just once, in March 2022. Thereafter,  $A$  and  $B$  were kept fixed during the experiment (i.e., no re-calibration was done afterwards).

### 3. Data analysis

This section presents the data analysis, including radiation background measurement, background subtraction, dead-time correction, and three different analysis methods we applied to look for deviations from normal exponential radioactive decay.

#### 3.1. Background measurement in JURLab

Shortly after setting up the detectors, the radiation background at Level -3 of JURLab had been measured before and

during Run-0. This 18-month dataset of 1-hour spectra samples was utilized to check the stability of the radiation background in the absence of any external radioactive sources. Figure 5 presents the main environmental components. One can clearly see that, in the interval between 100 keV and 2000 keV, the most remarkable decay lines come from  $^{235}\text{U}$ ,  $^{212}\text{Pb}$ ,  $^{214}\text{Pb}$ ,  $^{208}\text{Tl}$ ,  $^{214}\text{Bi}$ ,  $^{137}\text{Cs}$ ,  $^{228}\text{Ac}$ , and  $^{40}\text{K}$ . These sources originate from the architectural structure of JURLab (mostly concrete) and from the filtered air transferred by the HVAC system.

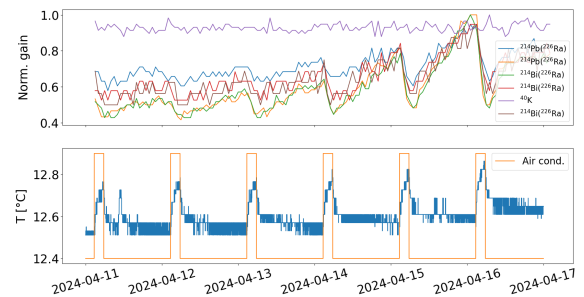


**Figure 6:** The relative activity of the daughters of  $^{222}\text{Rn}$ , and temperature,  $T$  at the JURLab Level -3, respectively.

The relationship between the change of the gain of the daughters of  $^{222}\text{Rn}$  and the variation of the physical

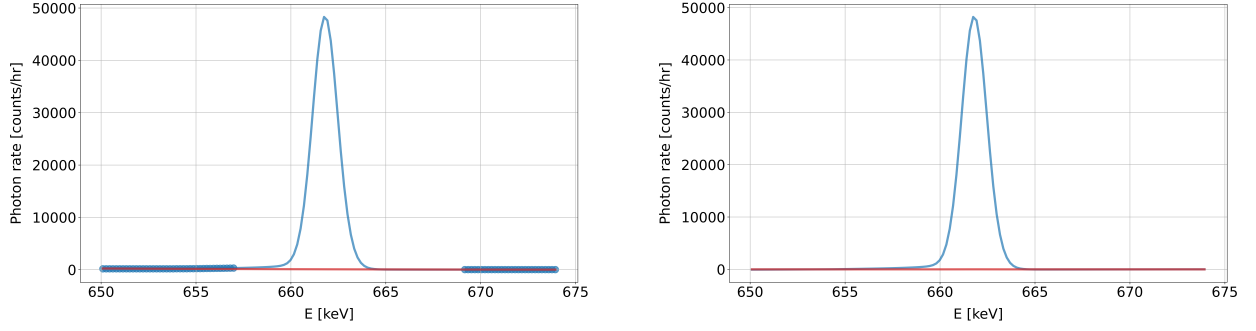


**Figure 7:** Left: The background near the  $^{137}\text{Cs}$  peak was fitted with a linear function. Only the data marked by blue dots were considered for fitting. The peak and its (arbitrarily chosen) immediate neighbourhood were excluded from fitting. Right: The peak and its neighborhood after background subtraction.

environmental parameters: Laboratory temperature,  $T$ . The time variation plots in Fig. 6 show the data of a period of 6 days after Run-4. For this test period the air conditioner worked for one hour each day. The gain of each isotopes were normalized to unity on the top panel. One can see that the daughters of  $^{222}\text{Rn}$  were effectively removed by the air conditioner while the activity of  $^{40}\text{K}$  remained within a narrow band. This is in clear coincidence with the on/off state of the HVAC system as plotted with yellow line in the bottom panel. A similar correlation is visible with the laboratory temperature,  $T$  (blue line) with respect to the HVAC "on" status with a slight increase and followed by a relaxation back to the "cellar" temperature after it is turned to "off" state.

### 3.2. Common analysis elements: background subtraction and dead-time correction

Background under the  $^{137}\text{Cs}$  peak in the measured raw spectrum was estimated by jointly fitting a quadratic polynomial of energy to the side bands [650,657] keV and [669, 674] keV (Fig. 7). After background subtraction, the total peak area was determined by using a Gaussian fit (for analysis methods 1 & 2) or via direct summation of signal counts (analysis method 3), in the full [650,674] keV range. To test the accuracy of background subtraction, we studied the variation in extracted peak area for integration range progressively narrowed by up to 30% (i.e., to [653.5,670.5] keV), and found less than 0.1% relative change in the peak area in all cases.

A dedicated setup for measuring dead time is not installed yet, so we relied on the live-time estimates,  $\Delta t_{\text{live}} = \Delta t_{\text{nominal}} - \Delta t_{\text{dead}}$ , provided by the Lynx analyzer (stored automatically in the recorded CNF datafiles). Background-subtracted peak areas were corrected for dead time by up-scaling to the nominal one-hour measurement duration by a factor  $\Delta t_{\text{nominal}}/\Delta t_{\text{dead}}$ .

### 3.3. Analysis method No. 1

In our first method, one-hour mini-run datasets were analyzed separately. After background subtraction,  $^{137}\text{Cs}$  peak areas were obtained and dead-time corrected. Finally,

individual peak areas from mini-runs were averaged for each month of the experiment (October 2022 through March 2023). Figure 8 shows the results of analysis method No. 1. A gradual decreasing trend is visible in the filled circles, corresponding to an exponential decay of the source activity. Given the approximately 30-year half-life of  $^{137}\text{Cs}$ , source activity is expected to weaken annually by  $\sim 1.1\%$  [32].

During a time interval  $[t, t + \Delta t]$  the average source activity, relative to the activity at time  $t_0$ , is

$$R(t, \Delta t | t_0) = \frac{1}{e^{-\lambda t_0}} \left[ \frac{1}{\Delta t} \int_t^{t+\Delta t} dt' e^{-\lambda t'} \right] = e^{\lambda(t-t_0)} \frac{1 - e^{-\lambda \Delta t}}{\lambda \Delta t}, \quad (2)$$

where  $\lambda \equiv \ln 2 / T_{1/2}$ . For each one-hour dataset, the measured activity, i.e., the extracted peak area was scaled to a common reference time  $t_0$  via dividing by  $R(t_{\text{nominal}}, \Delta t | t_0)$ . We set  $t_0$  to Oct 1, 2022. One can read result from Method No. 1. A  $\sim 0.2\%$  decrease is still visible after correction (squares). This likely reflects the limited accuracy of background subtraction and/or systematic error coming from the assumed Gaussian shape of the  $^{137}\text{Cs}$  peak vs. energy.

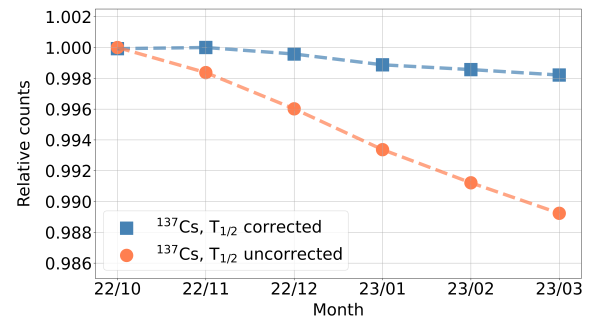


**Figure 8:** Results of analysis method No. 1.

### 3.4. Analysis method No. 2

As a crosscheck, a second analysis method was also investigated. Raw spectra from the one-hour mini-runs were

first summed for each month of Run-1, and background subtraction and area extraction were then performed using the monthly combined histograms. Results from the second method can be seen in Fig. 9. If one does not compensate for the exponential weakening of the source (filled circles), decreasing trend is manifest with magnitude similar to the one of the first method — albeit it does not look as smooth. It is again straightforward to compensate for the source half-life, considering that histograms contain monthly summed information in this case. One can use the ratio of the total uncompensated live time for the mini-run

$$t_{\text{live}}^{\text{TOT}} = \sum_i \Delta t_{\text{live},i}$$

where  $i$  indexes the mini-runs, and the decay-compensated total live time

$$t_{\text{live}}^{\text{TOT,comp}} = \sum_i R(t_i, \Delta t_{\text{nominal}} | t_0) \Delta t_{\text{live},i}$$

to correct extracted areas by a multiplicative factor  $t_{\text{live}}^{\text{TOT}} / t_{\text{live}}^{\text{TOT,comp}}$ . The trend becomes flatter. With the source half-life compensated for, but a  $\sim 0.4\%$  decreasing residual is still observable (Fig. 9). Just like for Method No. 1, Method No. 2 suggests that the dominant systematic errors that limit our accuracy come from background subtraction and/or the Gaussian shape assumption for the  $^{137}\text{Cs}$  peak.

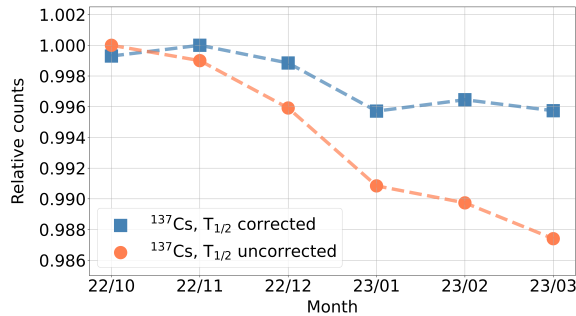


Figure 9: Results of analysis method No. 2.

### 3.5. Analysis method No. 3

The third analysis method we tried is similar to Method No. 2, except that - instead of Gaussian fitting - peak areas were obtained by simply summing the dead-time corrected and background-subtracted histograms in the energy range [650, 674] keV. Half-life uncorrected results shown from Method No. 3 in Fig. 10 look very similar to those from Method No. 1. Exponential decay in source activity can, of course, be compensated the same way as for Method No. 2. After such a correction, a weak 0.15% dropping trend still remains (Fig. 10, filled boxes).

Note, however, that the background fit can go negative. Setting negative contributions to zero in both background and the resulting background-subtracted histograms would give a somewhat higher overall yield and slightly larger

0.17% residual after source half-life correction (not shown). Yet again, this underscores that at present the main factor limiting sensitivity is the systematic error in background subtraction.

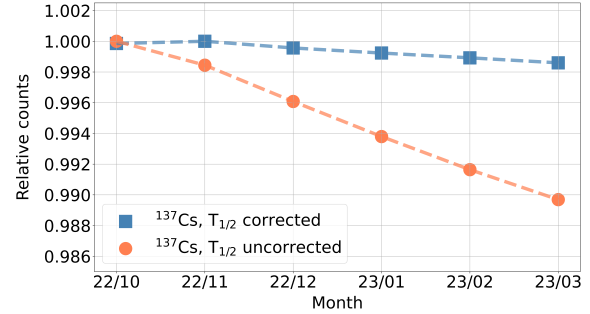


Figure 10: Results of analysis method No. 3.

## 4. Discussion and Conclusion

In this work we introduced an on-going radioactive decay measurement at the Jánossy Underground Research Laboratory of the HUN-REN Wigner Research Centre for Physics at Csillebérc, Budapest, Hungary. Key advantages of this underground facility are the low radiation background and the undisturbed physical environment. We presented a preliminary analysis of gamma spectra collected for an over 6-month period with a  $^{137}\text{Cs}$  radioisotope during run periods Run-0 and Run-1. We applied three different analysis methods to test the possible variation in the decay parameter, which was found to be  $\lesssim \mathcal{O}(\%)$ .

If one makes a "null-hypothesis" that  $^{137}\text{Cs}$  decays obey the pure decay exponential law, then our results corroborate that hypothesis to within a (relative) systematic error of a few *tenth* of a percent, which is indicative of our current experimental sensitivity. Our results also seem to be incompatible with an annual modulation in  $^{137}\text{Cs}$  decay rates that has a relative amplitude of a *few percent* or more — but we cannot rule out modulations of substantially smaller amplitude.

We hope to achieve significant improvements to the sensitivity of the measurement in the future via i) better shielding to reduce the background further, ii) improved methods for background subtraction and post-calibration of recorded data (Run-2, Run-3 and Run-4), and (iii) further long-term measurements.

## Acknowledgments

Instrument R&D and operation were done in the Jánossy Underground Research Laboratory (JURLab) of the Vesztergombi Laboratory for High Energy Physics (VLAB), Wigner Datacenter and the Wigner Scientific Computing Laboratory (WSCLAB) at HUN-REN Wigner Research Centre for Physics.

## References

- [1] D. Alburger, G. Harbottle, E. Norton, Half-life of  $^{32}\text{Si}$ , *Earth and Planetary Science Letters* 78 (1986) 168–176.
- [2] K. J. Ellis, The effective half-life of a broad beam  $^{238}\text{Pu}/\text{Be}$  total body neutron irradiator, *Physics in Medicine & Biology* 35 (1990) 1079.
- [3] E. D. Falkenberg, Radioactive decay caused by neutrinos.
- [4] A. Parkhomov, Deviations from beta radioactivity exponential drop, *Journal of Modern Physics* 2 (2011) 1310–1317.
- [5] P. A. Sturrock, E. Fischbach, J. H. Jenkins, Further evidence suggestive of a solar influence on nuclear decay rates, *Solar Physics* 272 (2011) 1.
- [6] J. H. Jenkins, E. Fischbach, Perturbation of nuclear decay rates during the solar flare of 2006 december 13, *Astroparticle Physics* 31 (2009) 407–411.
- [7] M. H. McDuffie, P. Graham, J. L. Eppel, J. T. Gruenwald, D. J. II, D. E. Krause, E. Fischbach, Anomalies in radioactive decay rates: A bibliography of measurements and theory, 2020.
- [8] G. T. Emery, Perturbation of nuclear decay rates, *Annual Review of Nuclear and Particle Science* 22 (1972) 165–202.
- [9] J. N. Bahcall, Theory of bound-state beta decay, *Phys. Rev.* 124 (1961) 495–499.
- [10] F. Bosch, T. Faestermann, J. Friese, F. Heine, P. Kienle, E. Wefers, K. Zeitelhack, K. Beckert, B. Franzke, O. Klepper, C. Kozhuharov, G. Menzel, R. Moshhammer, F. Nolden, H. Reich, B. Schlitt, M. Steck, T. Stöhlker, T. Winkler, K. Takahashi, Observation of bound-state  $\beta^-$  decay of fully ionized  $^{187}\text{re}$ :  $^{187}\text{re}-^{187}\text{os}$  cosmochronometry, *Phys. Rev. Lett.* 77 (1996) 5190–5193.
- [11] M. Jung, F. Bosch, K. Beckert, H. Eickhoff, H. Folger, B. Franzke, A. Gruber, P. Kienle, O. Klepper, W. Koenig, C. Kozhuharov, R. Mann, R. Moshhammer, F. Nolden, U. Schaaf, G. Soff, P. Spädtkke, M. Steck, T. Stöhlker, K. Sümmerer, First observation of bound-state  $\beta^-$  decay, *Phys. Rev. Lett.* 69 (1992) 2164–2167.
- [12] Y. A. Litvinov, F. Bosch, Beta decay of highly charged ions, *Reports on Progress in Physics* 74 (2010) 016301.
- [13] H. J. Assenbaum, K. Langanke, C. Rolfs, Effects of electron screening on low-energy fusion cross sections, *Zeitschrift für Physik A Atomic Nuclei* 327 (1987) 461–468.
- [14] F. Raiola, P. Migliardi, L. Gang, C. Bonomo, G. Gyürky, R. Bonetti, C. Brogini, N. Christensen, P. Corvisiero, J. Cruz, A. D’Onofrio, Z. Fülöp, G. Gervino, L. Gialanella, A. Jesus, M. Junker, K. Langanke, P. Prati, V. Roca, C. Rolfs, M. Romano, E. Somorjai, F. Strieder, A. Svane, F. Terrasi, J. Winter, Electron screening in  $d(d,p)t$  for deuterated metals and the periodic table, *Physics Letters B* 547 (2002) 193–199.
- [15] Y. Nir-El, G. Haquin, Z. Yungreiss, M. Hass, G. Goldring, S. K. Chamoli, B. S. N. Singh, S. Lakshmi, U. Köster, N. Champault, A. Dorsival, G. Georgiev, V. N. Fedoseyev, B. A. Marsh, D. Schumann, G. Heidenreich, S. Teichmann, Precision measurement of the decay rate of  $^7\text{Be}$  in host materials, *Phys. Rev. C* 75 (2007) 012801.
- [16] R. Schwengner, G. Rusev, N. Benouaret, R. Beyer, M. Erhard, E. Grosse, A. R. Junghans, J. Klug, K. Kosev, L. Kostov, C. Nair, N. Nankov, K. D. Schilling, A. Wagner, Dipole response of  $^{88}\text{Sr}$  up to the neutron-separation energy, *Phys. Rev. C* 76 (2007) 034321.
- [17] V. Kumar, M. Hass, Y. Nir-El, G. Haquin, Z. Yungreiss, Absence of low-temperature dependence of the decay of  $^7\text{Be}$  and  $^{198}\text{Au}$  in metallic hosts, *Phys. Rev. C* 77 (2008) 051304.
- [18] B. Wang, S. Yan, B. Limata, F. Raiola, M. Aliotta, H. W. Becker, J. Cruz, N. De Cesare, A. D’Onofrio, Z. Fülöp, L. Gialanella, G. Gyürky, G. Imbriani, A. Jesus, J. P. Ribeiro, V. Roca, D. Rogalla, C. Rolfs, M. Romano, D. Schürmann, E. Somorjai, F. Strieder, F. Terrasi, Change of the  $^7\text{be}$  electron capture half-life in metallic environments, *The European Physical Journal A - Hadrons and Nuclei* 28 (2006) 375–377.
- [19] T. Spillane, F. Raiola, F. Zeng, H. W. Becker, L. Gialanella, K. U. Kettner, R. Kunze, C. Rolfs, M. Romano, D. Schürmann, F. Strieder, The  $^{198}\text{au}$   $\beta$  half-life in the metal  $\text{au}$ , *The European Physical Journal A* 31 (2007) 203–205.
- [20] F. Raiola, T. Spillane, B. Limata, B. Wang, S. Yan, M. Aliotta, H. W. Becker, J. Cruz, M. Fonseca, L. Gialanella, A. P. Jesus, K. U. Kettner, R. Kunze, H. Luis, J. P. Ribeiro, C. Rolfs, M. Romano, D. Schürmann, F. Strieder, First hint on a change of the  $^{210}\text{po}$  alpha-decay half-life in the metal  $\text{cu}$ , *The European Physical Journal A* 32 (2007) 51–53.
- [21] E. Fischbach, V. Barnes, N. Cinko, J. Heim, H. Kaplan, D. Krause, J. Leeman, S. Mathews, M. Muetherthies, D. Neff, M. Pattermann, Indications of an unexpected signal associated with the gw170817 binary neutron star inspiral, *Astroparticle Physics* 103 (2018) 1–6.
- [22] E. Fischbach, J. B. Buncher, J. T. Gruenwald, J. H. Jenkins, D. E. Krause, J. J. Mattes, J. R. Newport, Time-dependent nuclear decay parameters: New evidence for new forces?, *Space Science Reviews* 145 (2009) 285–335.
- [23] E. Fenyvesi, G. G. Barnaföldi, G. G. Kiss, D. Molnár, Decay rate measurements with a  $^{137}\text{cs}$  radioisotope source at jánosy underground research laboratory (csillebéc, hungary), in: *Proceedings of Science*, number 441 in PoS(TAUP2023), p. 347.
- [24] T. N. Szegedi, G. G. Kiss, P. Mohr, A. Psaltis, M. Jacobi, G. G. Barnaföldi, T. Szücs, G. Gyürky, A. Arcones, Activation thick target yield measurement of  $\text{Mo}100(\alpha,n)\text{Ru}103$  for studying the weak r-process nucleosynthesis, *Phys. Rev. C* 104 (2021) 035804.
- [25] 2024.
- [26] D. Varga, G. Nyitrai, G. Hamar, G. Galgóczi, L. Oláh, H. Tanaka, T. Ohmimoto, Detector developments for high performance muography applications, *Nuclear Instruments and Methods in Physics Research Section A: Accelerators, Spectrometers, Detectors and Associated Equipment* 958 (2020) 162236. *Proceedings of the Vienna Conference on Instrumentation* 2019.
- [27] 2024.
- [28] L. Völgyesi, G. Szondy, G. Tóth, G. Péter, B. Kiss, G. G. Barnaföldi, L. Deák, C. Égető, E. Fenyvesi, G. Gróf, L. Somlai, P. Harangozó, P. Levai, P. Ván, Preparations for the remeasurement of the Eötvös Experiment, in: *Proceedings of International Conference on Precision Physics and Fundamental Physical Constants — PoS(FFK2019)*, volume 353, p. 041.
- [29] NNDC,  $^{137}\text{cs}$  data, 2024.
- [30] M. T. C. KK, Radioactivity measurement equipment, 2024.
- [31] M. TECHNOLOGIES, Lynx digital signal analyzer, 2024.
- [32] LNHB,  $^{137}\text{cs}$  basic data, 2024.